The variable European Little Ice Age

Heinz Wanner[1], Christian Pfister[1] and Raphael Neukom[2,3]

[1]Oeschger Centre for Climate Change Research, University of Bern, Bern, Switzerland
[2] Department of Geography, University of Zurich, Switzerland
[3]Department of Geosciences, University of Fribourg, Switzerland

Keywords
Holocene, Europe, Little Ice Age, Medieval Climate Anomaly, forcing factors, North Atlantic Oscillation, extreme events

Abstract

The Little Ice Age (LIA), which lasted from about 1250 to 1860 AD, was likely the coldest period of the last 8000 years. Using new documentary data and analyses of alpine glacier fluctuations, the complex transition from the Medieval Climate Anomaly to the LIA and the ensuing high variability of seasonal temperatures, are described and interpreted for Europe. The beginning of the LIA was likely different in both hemispheres. The low temperature average of the LIA is primarily due to the high number of cold winters. Conversely many summers were warm and dry.

Important triggers of the lower temperatures were, primarily, the numerous clusters of volcanic eruptions and the weak solar irradiance during the four prominent Grand Solar Minima: Wolf, Spörer, Maunder, and Dalton. The drop in temperature triggered the sea-ice–albedo feedback and led to a weakening of the Atlantic overturning circulation, possibly associated with a trend towards negative North Atlantic Oscillation indices.

The statistics of extreme events show a mixed picture. Correlations with forcing factors are weak, and can only be found in connection with the "Years without a Summer", which very often occurred after large volcanic eruptions.

1. Introduction

The term “Little Ice Age” (LIA) was first coined by Matthes (1939). He used it to refer to the resurgence of glaciers in the Sierra Nevada region of California in connection with the onset of cooling after the Holocene Thermal Maximum (Marcott et al., 2013; Kaufman et al., 2020). This cooling was primarily triggered by the decrease in solar insolation during the boreal summer, which can be attributed to the Earth’s orbital fluctuations (especially precession in combination with obliquity; Wanner et al., 2008). Based on their studies on glaciers in North America, Porter and Denton (1967) as well as Denton and Karlén (1973) called this process Neoglaciation. This term was generally accepted, and “Little Ice Age” was mostly used, especially after the fundamental publication by Grove (1988), for the massive glacier advances during the last millennium, which culminated with maximum glacier stages in numerous mountain regions of the Northern Hemisphere (Solomina et al., 2015). Since the term triggers associations with the main Ice Ages, it has been questioned by various authors (Landsberg, 1985; Bradley and Jones, 1992; Jones and Mann, 2004). The term has nevertheless caught on, and LIA was also used to describe the general decline in temperature, and further related to the associated consequences for agriculture and food availability (Le Roy Ladurie, 1971; Pfister, 2007).

The definitions for the beginning and end of the LIA differ considerably, depending on the region and dataset used. Table 1 shows a selection of time points for the beginning and end as more precisely defined in publications for different regions. According to this table the LIA in the Northern Hemisphere started between 1200 and 1400 AD. In the Southern Hemisphere the beginning of the LIA was delayed by about two centuries. This is probably related to the fact that temperature changes occurred later in the Southern Hemisphere because of the higher inertia due to the huge ocean areas (Neukom et al., 2014). In the European area the LIA ended with the last glacier advances around 1860, at the earliest, and likely a few decades later in the Southern Hemisphere (Pfister and Wanner, 2021). Carozza et al. (2015) show that the number of publications per year containing the term LIA has risen steadily since 1970, reaching almost 100 in the year 2000 and now significantly exceeding 500.

Table 1. Selection of time points for the beginning and end of the Little Ice Age in various publications.

Time period	Data source	Studied area	Reference
1200-1850	Tree rings	Northern Hemisphere extratropics	Esper et al., 2002
1250-1700	Tree rings, documents	Europe	Luterbacher et al., 2016
1250-1850	Different proxy types	Global	Wanner and Grosjean, 2014
1275/1300-?	Ice-cap expansion	Arctic Canada	Miller et al., 2012
1300-1800	Sediment analysis	Western Mediter-ranean area	Nieto-Moreno et al., 2013
1300-1800	Chironomids	Eastern Alps	Ilyashuk et al., 2019
1300-1850	Different proxy types	Iberian mountains	Oliva et al., 2018
1300-1900	Different proxy types	Northern Hemisphere	Ljungqvist, 2010
1359-1900	Different proxy types	Global	Büntgen and Hellmann, 2014
1375-1820	Varved lake sediments	Baffin Island, Canada	Moore et al., 2001
1400-1850	Speleothem	Central European Alps	Mangini et al., 2005
1400-1900	Different proxies	Northern Hemisphere	Mann et al., 2002
1450-1850	Different proxies	Global	IPCC ,2013
1490-1890	Sediment (plant remains)	Northwest China	Liu et al., 2010
1530-1900	Ice core	Peru	Thompson et al., 1992
1550-1850	Different sources	Global	Lamb, 1977
1550-1890	Sediment analysis	Southwest China	Chen et al., 2005

During the last 5000 years several cold relapses similar to the classical LIA occurred. Grove (2004) called them all “Little Ice Ages”. Matthews and Briffa (2005) proposed the term “Little Ice Age-Type Events” (LIATE) for these glacial advances which lasted decades to centuries. Typical examples are the cold relapses between about 3500 and 3100 years BP (also called Loebben oscillation in the European Alps; Mayr, 1964), the so-called “2.8 kyr BP event” (also called Homeric Minimum or Göschenen cold phase I; Martin-Puertas et al., 2012) and the “Dark Ages or Migration Period Pessimum” between about 540 and 900 AD (also called Göschenen II cold phase; Helama et al., 2017). Büntgen et al. (2016) have coined the term Late Antique Little Ice Age (LALIA) for this period. They have shown that the cold regression after the volcanic eruptions of 536, 540 and 547 was very massive and occurred much more rapidly than in the case of the LIA. The expression LIATE was used in a different way by Wanner et al.

(2000). These authors used this term to define the quasiregular glacier advances during the Little Ice Age. Three striking events were observed in the European Alps around 1370, 1680 and 1860 AD (Fig. 1f).

In this paper we investigate the structure of the European LIA using annual mean and seasonally reconstructed temperature indices as well as selected glacial curves. They are interpreted based on temperature trends, forcing factors and internal variability. At the end we focus on the temporal sequence of extreme events.

2. LIA climate

Under the keyword "Holocene temperature conundrum" it is still discussed whether the last 5000 years showed a positive or negative temperature trend (Liu et al., 2014; Kaufman et al., 2020; Osman et al., 2021; Wanner, 2021). Reconstructions demonstrate that the above-mentioned cold phases during the late Holocene, which led to glacial advances, were repeatedly interrupted by warmer periods with glacier retreat phases, such as the Bronze Age Warming Period or the Iron/Roman Age Warm Period (Pfister and Wanner, 2021).

Figure 1a shows two temperature time series, which were determined by two different statistical methods described in the paper of Luterbacher et al. (2016). Both curves were reconstructed by using tree-ring and documentary data. They therefore represent central European summer land temperatures (with respect to the 1500–1850 AD mean). As Table 1 has already shown, it is not possible to specify an exact start of the LIA, and the transition from the Medieval Climate Anomaly (MCA) or Medieval Warm Period (MWP; Crowley and Lowery, 2000; Bradley et al., 2003; Diaz et al., 2011) to the LIA shows a complex pattern. It took place in several stages and was more like a gradual "settling in" than a clear linear transition.

The European summer warming between 1125 and 1225 AD (Fig. 1a) was likely a last "heat pulse" of the MCA. Accordingly, based on this curve, the beginning of the LIA could be fixed at about 1250 AD. Despite the complex structure it can be clearly established that the annual mean temperatures of the LIA were relatively low from this date until the turn from the 19th to the 20th century. Four notable cold episodes occurred around 1460, 1600, 1690 and 1825 AD. Almost no high resolution proxies are available for winter temperatures from natural archives, in contrast to evidence from archives of society (Fig. 1b).

The seasonal transition from the MCA to the LIA is demonstrated by the four time series of the Figures 1b-e. They represent smoothed curves of the Pfister-Indices, which were determined for each season of the last 1000 years, insofar as sufficient sources were available (Pfister and Wanner, 2021). The generation of indices is a customary approach in historical climatology to transform raw weather descriptions into semi-quantitative ordinal data. The Pfister temperature and precipitation index is the most widely used in the world (Nash et al., 2021). It classifies the temperatures of each season into seven classes from -3 (very cold) to +3 (very warm). The method is described in depth in Pfister et al. (2018). A shorter description is presented in the annex of this article. The information refers to an area that mainly comprises Germany, Switzerland and the Czech countries. For the period up to 1499 Pfister-Indices for very cold and very warm winters and summers (Index >1 and <-1) are individually documented. Thereby, the narrative evidence is based on reliable compilations and the proxy data draw on calibrated documentary evidence. The indices from 1500 to 1759 were determined based on estimates by Dobrovolný et al. (2010) and subsequently on instrumental observations. These authors demonstrated that the documentary evidence explains a large fraction of temperature variability, varying according to season (from 73% in autumn to 83% in winter). The series are significantly correlated to 91% of all grid cells in the entire European and northern Mediterranean temperature field (Luterbacher et al. 2010).

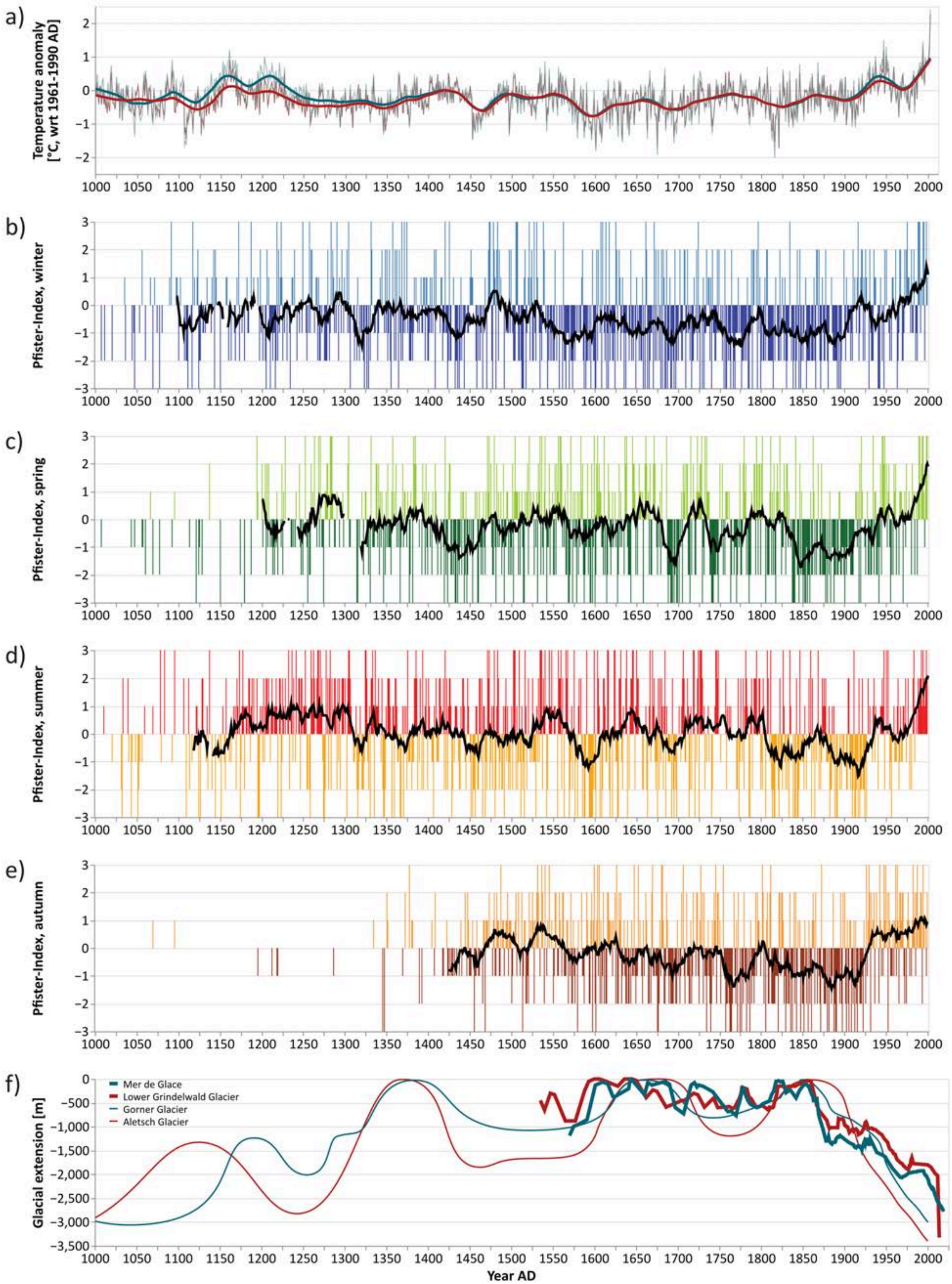

Figure 1. a) Two reconstructions of the European summer temperature anomalies with respect to 1500–1850 AD (detailed description in: Luterbacher et al., 2016). b-e) Seasonal Pfister Indices for the last millennium. The black curve shows the mean for a 21 years long moving window. f) Fluctuations of four Alpine glaciers, reconstructed based on different data sources with different time resolution (tree rings, fossil soils and documents; Holzhauser et al., 2005; Holzhauser, 2010; Nussbaumer et al., 2016).

In Figures 1b-e the MCA–LIA transition becomes roughly visible, especially in the winter and summer seasons, whose reconstructions are based on the most complete evidence by far. During the winter season there were already significant drops in temperature during the 12th century and, compared to summer, the seasonal picture clearly shows that the LIA was primarily a winter phenomenon. Mostly cold winter conditions prevailed from 1300 AD to the early 20th century. The primary importance of winter temperatures is also confirmed by a study from Jones et al. (2014) for the Northern Hemisphere north of 30°N. During the other three seasons, periods of several decades with lower temperatures were repeatedly interrupted by warmer phases. In the summer half-year, a cold relapse around 1150 AD was followed by a long period of about 130 years with many warm summers. Longer warm summer periods also occurred around 1550, 1640, 1730, 1790 and 1870 AD. These facts underscore that only averaging over a longer time period of several centuries indicates the general character of the MCA and the LIA. Lamb (1965) drew heavily on Viking voyages and accounts of the fertile 13th century in describing the "Medieval Warm Epoch", and Matthes (1939), by defining the LIA, was clearly influenced by the striking glacial advances.

Glaciers excellently reveal the course of the climate over decades to centuries. The mass balance of the ice responds to fluctuations in the radiation balance and temperature, but also in solid precipitation. Summer temperatures and the summer snowfall, which changes the albedo of the glacier surface, are of primary importance. Oerlemans (2005) has reconstructed the summer temperature signal using the mass balances of 169 glaciers. Overall, however, the glaciers react quite differently in different time periods, since the mass increase of snowfall in winter plays a decisive role (Reichert et al., 2001; Steiner et al., 2008). Depending on their size, glaciers have various reaction times. Figure 1f shows the fluctuations of four Alpine glaciers: one in the west (Mer de Glace) and three in the central Alps (see the map on Fig. 4 b). With a length of more than 20 km and ice thicknesses of up to 800 m, the Great Aletsch Glacier is the largest glacier of the European Alps. It covers an area of about 80 km^2, contains more than 20% of the total ice volume still present in the Swiss Alps (Jouvet and Huss, 2019) and is expected to recede with a time delay of more than half a century to climate fluctuations. This means that the Great Aletsch Glacier integrates decades-long temperature and precipitation changes. The Gorner Glacier in the Monte Rosa massif near Zermatt is about 12.4 km long (2014), and the 7 km-long Mer de Glace, located in the Chamonix Valley, is France's largest glacier. The Lower Grindelwald Glacier was about 8.3 km long in 1973 and by 2015 had shrunk significantly to just 6.2 km (Fig. 4b).

In Figure 1f, a first, smaller glacier advance prior to the LIA is shown for about 1120 (Great Aletsch Glacier) and 1180 AD (Gorner Glacier). The following long and warm summer periods during the 13th century are likely mirrored in a clear glacier retreat culminating around 1250 AD. The period of the LIA is clearly represented by three maximum glacier levels at about 1380, 1680 and 1860 AD. A larger retreat period occurred between 1500 and 1570 AD. The two shorter curves on Figure 1f, representing the glacier movement of the Lower Grindelwald Glacier and the Mer de Glace, were reconstructed with the help of documents (mainly drawings and paintings) and field findings (Nussbaumer et al., 2016). Both glaciers are smaller than the Great Aletsch Glacier. Based on the higher number of data sources, their reaction can be determined with a higher time resolution of several years or a decade. Unsurprisingly, the last two major advances of the Little Ice Age occurred earlier than in the larger Great Aletsch Glacier and the Gorner Glacier, and two additional advance phases stand out in the 18th century. After 1860 AD at the latest, a massive melting process with glacier retreats began in practically all Alpine glaciers (Pfister and Wanner, 2021).

3. LIA forcing and internal variability

At the millennial scale the energy balance and temperature of the late Holocene are decisively influenced by orbital forcing (Wanner et al., 2008). In Europe, summer insolation at 60°N decreased by a maximum of about 40 W/m^2 from the mid to the late Holocene due to the Earth's orbital variations, mainly influenced by precession and obliquity (Lorenz et al., 2006; Wanner et al., 2008; Marcott et al., 2013; Wanner, 2021). Conversely, however, it increased in winter, but by a small amount of about 3 W/m^2 (Wanner, 2021). This strong insolation decline in the boreal summer and the associated feedbacks (e.g. ice-albedo feedback) have formed the backdrop, so to speak, for the climate progression from the MCA to the LIA; however, the transition was very complex and other factors undoubtedly played an important role.

Figure 2 provides an overview of the influences of the annual to decadal scale climate forcing and internal (stochastic) variability on the European climate system during the last 1000 years. Groups of volcanic events and periods of Grand Solar Minima are shown in green and red bars (Figs. 2a and b). Their length is indicated in the annex. Three different horizontal bars show the results of reconstructions of the state of the North Atlantic Oscillation (NAO; Fig. 2d)**.** Based on a smoothing with a 21 year long moving window the periods with a positive NAO state were shown in red and those with a negative state in blue.

The smaller advance of the Great Aletsch and Gorner glaciers prior to the LIA (Fig. 1f), indicating cooling, occurred shortly before the longer warm pulse in summer temperatures from 1150 to 1250 AD (Fig. 1a; Holzhauser et al., 2005). It was likely influenced by the Oort Grand Solar Minimum (GSM; Fig. 2b). GSMs are responsible for both top-down and bottom-up effects on climate (Moffa-Sánchez et al., 2014). The top-down effect includes the decrease of ultraviolet radiation, which reduces the stratospheric ozone concentration and leads to a weakening of the stratospheric westerly jet, mainly in winter (Scaife et al., 2005; Meehl et al., 2013; Anet et al., 2013; Maycock et al., 2015). Therefore, easterly winds with cold-air advection occur more frequently in the lower troposphere, and the pressure distribution corresponds more or less to the pattern of a negative NAO (Wanner et al., 2001). The bottom-up process includes decreasing temperatures in the upper ocean (White et al., 1997) and over the continents (Ineson et al., 2015). The lower troposphere over the continents cools down by several tenths of a degree (Dobrovolný et al., 2010). The cooling prior to 1150 AD (Fig. 1a) was probably also influenced by the eruption of several volcanoes after 1000 and 1100 AD, including the Hekla in Iceland in 1104 (Fig. 2a). Figures 3a and 3b show the relative occurrence of the individual Pfister indices during the Grand Solar Minima. As expected, the Pfister indices related to Central Europe only react to the global solar forcing to a limited extent. Nevertheless, the summer values show a tendency to negative values. In winter, the high number of +2 values is surprising.

The three main advances of the Great Aletsch and Gorner glaciers, which occurred around 1380, 1680 and 1860 AD (Fig. 1f; Holzhauser et al., 2005), mark the classical duration of the LIA in Central Europe. Based on the temperature curves and the course of the glaciers in Figure 1, one could speak of a preliminary and a main phase of the European LIA. Usually the onset of the LIA is associated with reduced solar irradiance and enhanced volcanic activity, amplified by ocean–atmosphere–sea-ice feedbacks in the Northern Hemisphere, and a decrease in warm water supply within the subpolar gyre (SPG; Miller et al., 2012; Bradley et al., 2016). The preliminary phase of the glacier advance around 1380 AD was significantly influenced by two groups of volcanic events around 1200 and 1260 (Fig. 2a; Miller et al., 2012), including the eruption of Samalas in Indonesia around 1257, the largest volcanic event of the last 1000 years (Sigl et al., 2015; Toohey and Sigl, 2017). The huge aerosol masses emitted into the stratosphere by volcanoes absorb the short-wave solar radiation, which leads to warming there and to cooling on the ground and in the atmospheric boundary layer. This process affects the atmospheric circulation and thus the transport of energy and moisture (Robock, 2000). Especially the summers are cool and characterised by many days with precipitation, which is why they are referred to as "Years without a Summer" (Pfister and Wanner, 2021). Such cool and wet summers in company with cool, snowy winters are the main important ingredients of positive glacier mass balances (Reichert et al., 2001; Steiner et al., 2008), and their occurrence is often one of the most important triggers for the massive glacier advances during the LIA.

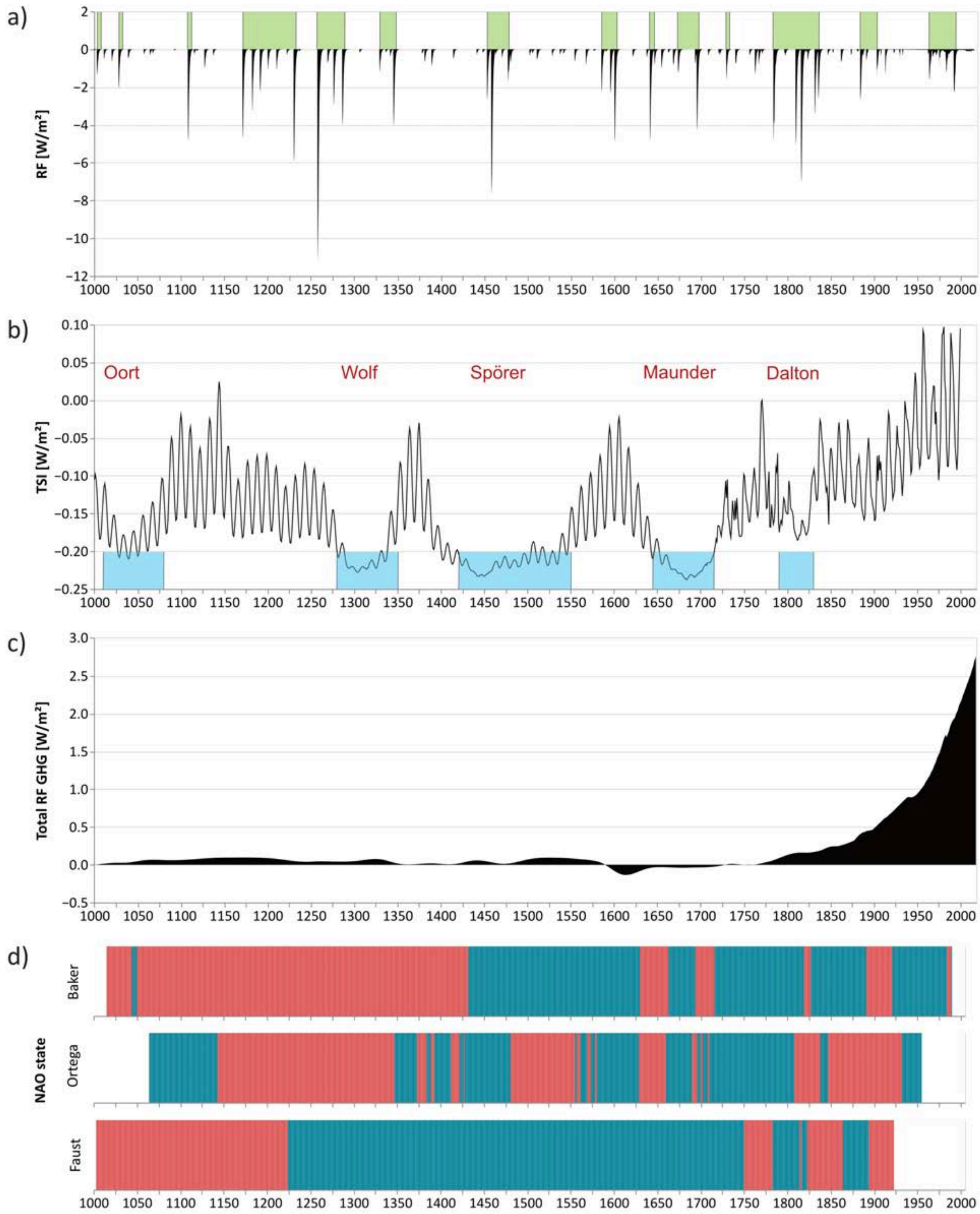

224 **Figure 2.** Significant parameters indicating forcing or internal variability of the European climate system during the last 1000 years. a) Reconstructed aerosol forcing mainly representing volcanic eruptions (with respect to 1950–2000; Toohey and Sigl, 2017). Groups of volcanic events are marked in green bars. b) Total solar irradiance (Muscheler et al., 2007; Usoskin et al., 2014). Grand Solar Minima are marked in blue bars. c) Total radiative forcing by the greenhouse gases CO2, CH4 and N2O (data sources: Ed Dlugokencky and Pieter Tans, NOAA/ESRL: www.esrl.noaa.gov/gmd/ccgg/trends/ as well as ftp://ftp.cmdl.noaa.gov/hats/N2O/combined/HATS_global_N2O.txt). d) Periods with a majority positive (red) or negative (blue) state of the NAO, shown for three different reconstructions (Baker et al., 2015; Ortega et al., 2015; Faust et al., 2016). The representation of annual time series is based on a smoothing with a 21 year long moving window.

This fact is also indicated by the Figures 3c and 3d which show the results of a Superposed Epoch Analysis for volcanic events, adjusted to the Pfister-Indices according to Figure 1a and c. The winter indices show almost no clear tendency. This is not surprising given the limited information of the available sources and the forcing data. In contrast, the summer indices indicate that more cold summers can be expected within the first three years after volcanic events.

Prior to the 1380 glacier advances, a series of cool and likely wet "Years without a Summer" occurred (Figs. 1d and 5b), and the winters, springs and summers were remarkably cold after 1300 (Fig. 1b-d). Numerous publications demonstrate the complexity of the MCA-LIA transition and especially the importance of the North Atlantic freshwater formation and the dynamics of the subpolar gyre (SPG). Based on data of the last decades already Dickson et al. (1988), Mysak et al. (1990), Aagard and Carmack (1989) as well as Walsh and Chapman (1990) pointed to the significant influence of the freshwater flux from the North European land mass into the polar basin, which influences the rate of deep convection in the high-latitude North Atlantic and, therefore, the thermohaline circulation. Ogilvie and Jónsson (2001) assumed that the LIA was triggered by the presence of polar waters, which also led to a modification of the atmospheric circulation. Lehner et al. (2013) argued that a sea-ice-ocean-atmosphere feedback, triggered by a reduction of the northward ocean heat transport, amplified the cooling at the beginning of the LIA in the North Atlantic – European region. Moffa-Sánchez et al. (2014) showed that the increasing amount of polar freshwater led to a reduced formation of Labrador Sea Water inducing the onset of the LIA cooling. Alonso-Garcia et al. (2017) also pointed out the importance of the Labrador Sea. They demonstrated that the warm climate of the MCA may have enhanced iceberg calving along the SE Greenland coast, and, as a result, freshened the SPG. Due to the resulting reduction of convection in the Labrador Sea, the North Atlantic circulation weakened, the heat transport to the high latitudes decreased, the atmosphere was cooling and the sea ice was growing. During the whole LIA this process was further enhanced by volcanic and solar forcing. Moreno-Chamarro et al. (2017) showed that, during winter, the LIA was amplified by sea-ice expansion and reduced heat losses in the Nordic and Barents seas, driven by a multi-centennial reduction in the northward heat transport of the SPG. Slawinska and Robock (2018) argued that large volcanic forcing is necessary to explain the origin and duration of LIA–like perturbations in the Last Millennium Ensemble simulations. They emphasized that other forcings might play a role as well. In particular, prolonged fluctuations in solar irradiance associated with solar minima potentially amplify the enhancement of the magnitude of volcanically triggered anomalies of Arctic sea ice extent. Miles et al. (2020) argued that sea-ice export and freshwater export from the Arctic Ocean, which commenced abruptly around 1300 AD and ended in the late 1300s, initiated the abrupt onset of the LIA. They questioned whether additional forcing by volcanoes or a weak sun were necessary at all for this process. Lapointe and Bradley (2021) provided a plausible explanation for the warming after 1350 AD (Fig. 1a), the subsequent glacial retreat after 1400 AD (Fig. 1f), and the onset of the principal phase of the European LIA. They showed that the index of ocean surface temperature variability (SST), called Atlantic Multidecadal Variability (AMV; Sutton et al., 2018), was clearly positive between 1320 and 1380 AD. This led to a persistent atmospheric blocking, linked to unusually high solar activity, triggering the intrusion of warm Atlantic water into the Nordic seas, followed by a breakup of sea ice and the calving of tidewater glaciers. The meltwater production weakened the SPG, setting the stage for the following long-term cooling during the main period of the European LIA.

The definitive transition to main phase of the European LIA took place with the Wolf and Spörer GSM, which occurred at short intervals (Fig. 2b, 5d). Both were accompanied by clusters of volcanic eruptions after 1450, around 1600 and before 1700 AD (Fig. 2a, 5c). These forcings decisively contributed to the second LIA glacial advances of the Great Aletsch and Gorner glaciers in 1680 AD. These advances, resolved into much more detailed movements, can also be recognised in the form of massive growth rates at Mer de Glace and Lower Grindelwald Glacier (Fig. 1f). This example clearly indicates that the longer cooling phases of the LIA are usually triggered by clusters of volcanic eruptions coinciding with a GSM (Bradley et al., 2016) and amplified by internal variability in the form of feedbacks involving atmosphere, ocean and sea ice. If there are hardly any volcanic events, and if solar activity remains constant at a medium level, temperatures will be higher. Typical examples are the early period of the Roman Empire (Büntgen et al., 2016) or the MCA (Diaz et al., 2011). The autumn months around 1450, in particular, were very cool (Fig. 1c), but mainly the summers before 1600 AD had low temperatures (Fig. 1d). From 1500 onwards, winters were almost continuously cold (Fig. 1b). These seasonal minima provide further evidence of the second LIA glacial advances during the 17th century (Fig. 1f), which culminated in the maximum glacier positions of the Great Aletsch and Gorner glaciers during the cold Maunder Minimum around 1680 AD.

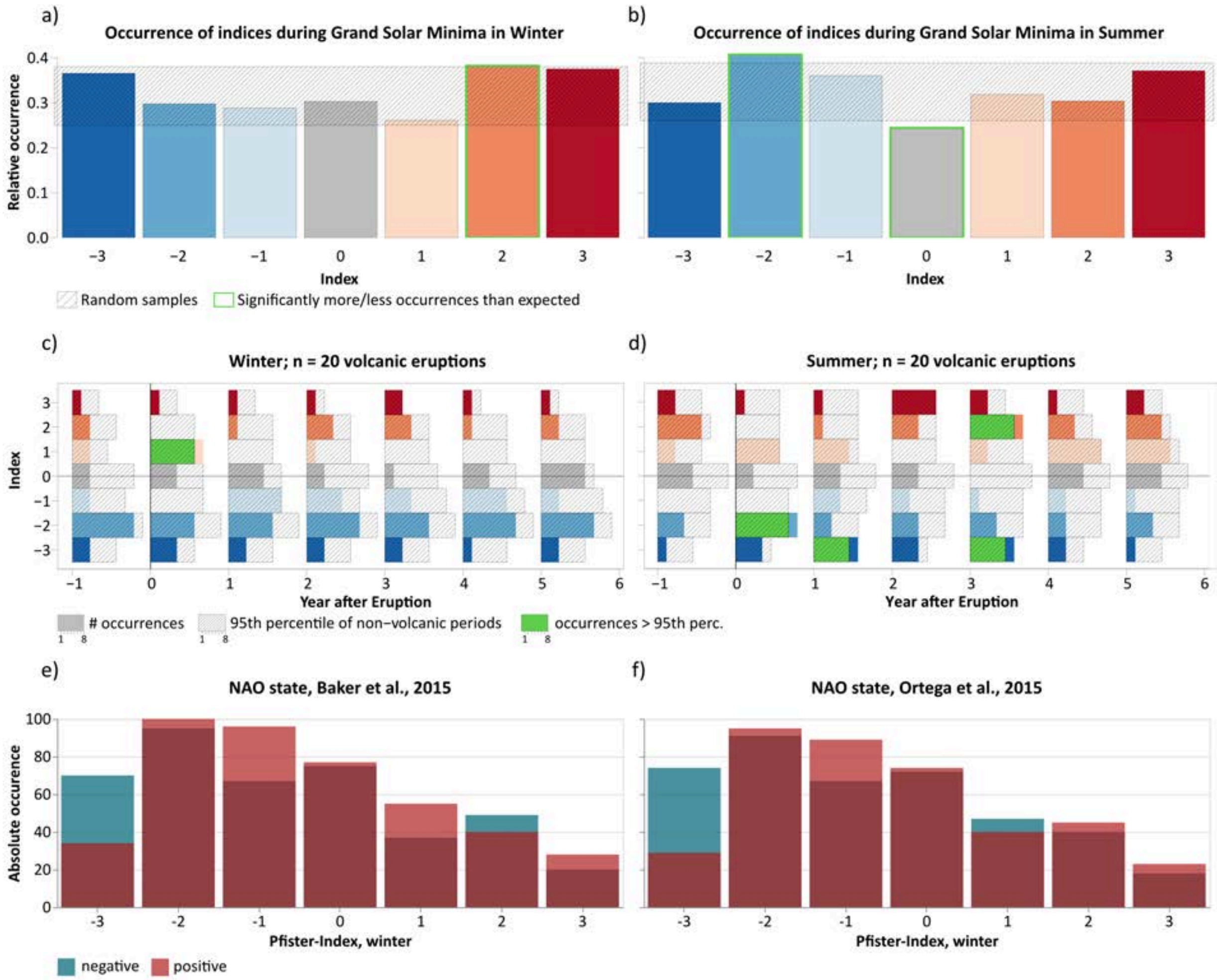

Figure 3. a and b) Relative occurrence of each temperature index during Grand Solar Minima (GSM). The number, each index occurs during GSM is divided by the total number of occurrences during the last millennium. Shaded box shows the 95% range of Monte-Carlo sampled periods of the same length as the GSM. Values that are outside the shaded range are marked in green. If the box is below the shaded range, this index occurs less frequently during GSM than expected by chance, and more frequently during non-GSM periods. If the box is above the shaded range, the index occurs more frequently during GSM than expected by chance and less frequently during non-GSM periods.
Fig. 3c and 3d) Superposed Epoch Analysis of the occurrence of each temperature index after large volcanic eruptions. For each index (y-axis) the number of occurrence in the years after the eruptions (x-axis) is shown as a colored box (red for warm temperatures, blue for cold temperatures). The width of each box represents the number of times the index occurs in this year. Shaded boxes represent the 95th percentile of occurrences during randomly sampled non-volcanic periods. If an index occurs more often than expected by chance, the 95th percentile is coloured in green. The analysis is conducted using the 20 largest eruptions of the last millennium. The vertical black line represents the eruption year.
Fig. 3e and 3f) Frequency distribution of the Pfister-Indices in winter and summer, divided into two categories with a positive (red) or negative (blue) NAO state. Overall, a negative NAO state is clearly dominated by clearly negative values (-3), which indicate very low temperatures.

Another conceivable forcing factor would be the influence of land use. However, there are hardly any studies that can experimentally prove the long-term influence of land use on temperature. Owens et al. (2017) have estimated this influence for the entire Northern Hemisphere based on simulations of the CESM Last Millennium Ensemble (Otto-Bliesner et al., 2016). They find that a slow, but near-continual cooling trend of about 0.2 °C occurred due to the removal of natural land cover (e.g. forests) producing a higher albedo effect.

Temperature, precipitation, and glacier behaviour are decisively co-determined by internal variability (Deser et al., 2010), which manifests in the form of interactions between ocean, atmosphere and land (including vegetation). In Europe, internal climate variability is mainly expressed in the form of NAO (Wanner et al., 2001). The influence of ENSO (El Niño Southern Oscillation) is definitely weaker (Brönnimann et al., 2007). Longer series of negative NAO indices indicate cold winters with frequent easterly flow and suppression of the westerlies. In contrast, positive indices point to increased westerlies and thus warmer and wetter winters, especially in the northern part of Europe. Hernandez et al. (2020) point to the fact that different NAO reconstructions produce divergent results. It must be assumed that the so-called NAO indices also show a large interannual and interdecadal variability.

Figure 2d shows the 1000-year course of the NAO state based on filtered data from three different reconstructions (Baker et al., 2015; Ortega et al., 2015; Faust et al., 2016). Various publications emphasise that the NAO indices were mostly positive during the MCA (Wassenburg et al., 2013) and mostly negative during the LIA (Wanner et al., 2001; Trouet et al., 2009; Baker et al., 2015; Hernández et al., 2020). This is only partially confirmed by the three time sequences shown in Figure 2d. Olsen et al. (2012) state that that the dominant atmospheric circulation pattern changed to negative NAO indices and became more variable during the LIA, and Copard et al. (2012) confirm that a negative mean NAO state during the LIA was connected to weaker und more southerly located westerlies and a westward contraction of the SPG. Based on their yearly NAO reconstruction which was validated with six model simulations (Fig. 3d) Ortega et al. (2015) find no persistent positive NAO during the MCA, but positive phases during the 13th and 14th centuries with remarkable warm periods in Winter, spring and summer. Lehner et al. (2012) demonstrated that, during the MCA, the European region was dominated by a persistent positive phase of the NAO, followed by a shift to a more oscillatory behaviour during the LIA. Based on a tree-ring based reconstruction Cook et al. (2019) emphasise that the NAO indices behave like a "white noise" process which is mainly stochastically forced. After all Figure 1d shows, from the 15th century onwards, mainly negative values dominate.

Figures 3 e and f show the distribution of the Pfister-Indices for two different time series of NAO indices (Baker et al., 2015 and Ortega et al., 2015), each divided into the distributions for positive (red) and negative values (blue). Both figures clearly show a dominance of very cold winters with index -3 in the case of a negative NAO state.

The seasonal Pfister Indices of the 18th century show considerable fluctuations, especially in winter, spring and autumn (Fig. 1b, c and e), which are manifested by two distinct advances in the smaller, rapidly reacting glaciers in Figure 1f. A mostly negative NAO state existed in the second half of this century (Fig. 1d). These events were followed by the Dalton GSM (Fig. 2b) and at least four large volcanic eruptions between 1808 and 1835 (Fig. 2a), above all the Tambora in 1815 (Sigl et al., 2015), which definitely triggered the third, large glacial LIA advance of the Great Aletsch and Gorner glaciers in 1860 AD (Holzhauser et al., 2005). At Mer de Glace the maximum glacier level was reached around 1821 (Le Roy Ladurie, 2012). The maximum levels of the 19th century are comparable to those around 1680 and 1380 AD (Fig. 1f). Together with the approximately similar advances around 500 AD (Braumann et al., 2021), they represent the maximum glacier levels of the Holocene. Figure 4a shows possibly the oldest photograph of the Lower Grindelwald Glacier, taken by the Bisson brothers in 1855/56 (Zumbühl et al., 2008). It shows, with high probability, the 19th-century maximum (Zumbühl, 2016). Cooling, which triggered the volcanic eruptions, also led to a weakening of the global monsoons as well as to a more southern position of the North Atlantic storm track (Brönnimann et al., 2019). The resulting higher precipitation amounts additionally contributed to glacier growth.

After 1860 AD, there was a marked glacier retreat of the Alps, the Cantabrian Mountains and the Sierra Nevada (Fig. 1f; Oliva et al., 2018). In the European Alpine region, too, various factors were held responsible for this rapid retreat. Both the annual mean temperatures (Fig. 1a) and especially the summer temperatures (Fig. 1d) indicate rising values. This temperature increase is likely due to the fact that there was only one volcanic eruption during the second half of the 19th century (Krakatoa in 1883), and that solar irradiance remained stable at an average level (Fig. 2b). In addition, the concentrations of greenhouse gases were already rising slightly (Fig. 2c). One exception is the winter temperature, which remained low. This cold was associated with drought (Steiner et al., 2005), which prevented a progression of positive mass balances of the glaciers. Finally, Painter et al. (2013) hypothesised that the retreat of glaciers in the European Alpine region was largely due to the increase in industrial black carbon and the associated changes in albedo. Their results were questioned by Sigl et al. (2018), who hypothesised that glacier length changes throughout the past 2000 years have been forced predominantly by summer temperature reductions induced by sulphuric acid aerosol forcing from large volcanic eruptions.

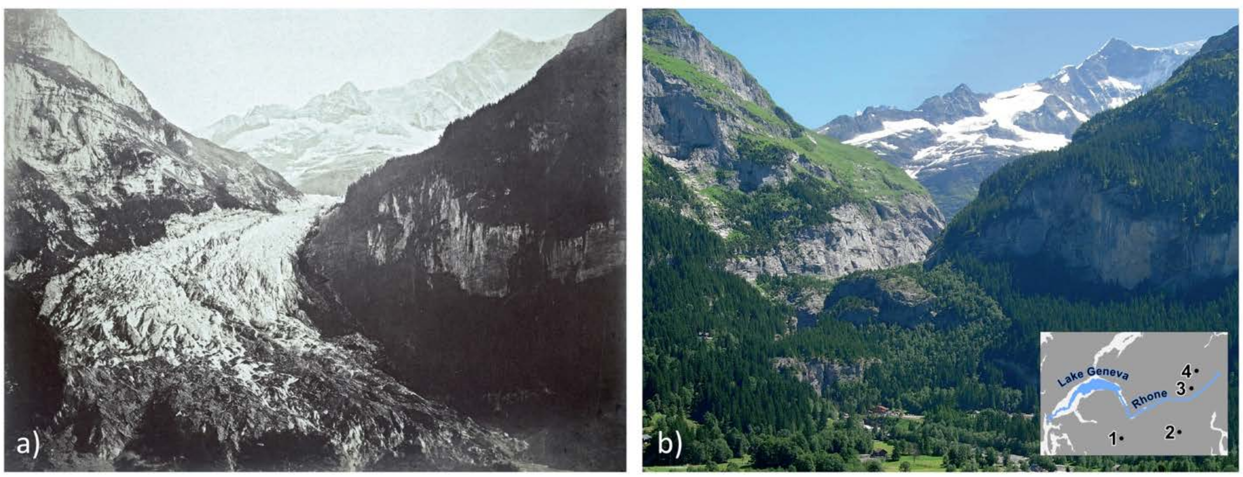

Figure 4. a) The advancing Lower Grindelwald Glacier, photographed by the brothers Louis Auguste and Auguste Rosalie Bisson during its greatest extent around 1855/56 AD (Zumbühl, 2016). b) The melting Lower Grindelwald Glacier, photographed by S. Nussbaumer on 2 August 2013 (Nussbaumer et al., 2016). The small map in the lower right corner of the Figure shows the locations of the four Alpine glaciers described in this paper: 1) Mer de Glace. 2) Gorner Glacier. 3) Great Aletsch Glacier. 4) Lower Grindelwald Glacier.

After a cold spell at the turn of the 20th century, which lasted until about 1920, a first warm phase occurred from 1943 to 1951, including the hot and dry summer and autumn of 1947 (Pfister and Wanner, 2021). It is significant that both solar irradiance (Fig. 2b) and the concentration of greenhouse gases followed a clearly positive trend during this period. Figure 4b, showing the Lower Grindelwald Glacier on 2 August 2013 (Nussbaumer et al., 2016), documents the fact that Alpine glaciers have been melting since 1860 at a rate that was probably never reached in the Holocene. The question is open whether the North Atlantic Oscillation has also had an effect on the dynamics of the glaciers. Its values were clearly in the positive range in the 1920s and between 1960 and the mid-1990s (Pinto and Raible 2012).

The LIA's "last signs of life" – the cold winters of 1956 and 1963 – were partly supported by volcanic events. From 1988/89, the European climate system started to follow a "new regime", so to speak, with significantly higher temperatures and dry phases, interrupted by sequences of heavy precipitation (Pfister and Wanner, 2021).

4. LIA extreme events

Climate extremes are hard to interpret and predict because they obey different statistical laws than averages (Naveau et al., 2005). Their rare occurrence makes it difficult to identify a trend. In this paper the events with a Pfister Index of -3 (extreme coldness) or +3 (extreme warmth) are defined as extreme. In Figures 5a and b, extreme winters and summers are documented for the last millennium. The most extreme events are marked with their corresponding year. Figures 5c and d represent the two significant climate forcings already depicted in Figure 2: clusters that mark several volcanic events which occurred in a short time period (green), and the five GSMs of the last millennium (blue; Oort, Wolf, Spörer, Maunder, and Dalton). The lowest bar (Fig. 5e) marks the three periods with a positive (red) or negative (blue) state of the North Atlantic Oscillation (NAO; Wanner et al., 2001; Baker et al., 2015).

Winters in which, at most, sporadic frost or snowfall and spring vegetation are described are rated as extremely warm (Index +3; upper, red series of dots in Fig. 5a). In the 12th century, three extremely warm winters are documented. The 13th to 15th centuries had six each, the 16th century eight, and the 17th century seven. In the following period, documented by using instruments, such extreme winters have occurred only once or twice per century until the transition to rapid warming in the 1980s. The warmest of all warm winters documented so far was in 1290. An anonymous monk, using careful observations of weather and vegetation, wrote that the trees in Colmar, France, had not yet shed their leaves by the beginning of January (according to Gregorian calendar), and new shoots were already sprouting. In England, not a single snowfall was recorded. In mid-February, fruit trees in Vienna were in full bloom as if it were May (Pfister and Wanner, 2021). Extreme warm winters are recorded sporadically until around 1700 and only sporadically between 1800 and 1987. Pfister and Wanner (2021) as well as the results in Figure 3a and b show that at primarily correlations with volcanic or solar irradiance forcing exist.

The most frequent severe winters (Index -3; lower, blue series of dots in Fig. 5a) occurred in the periods 1110–1150, 1205–1216 and 1323–1328. In between, there are longer periods without such events, especially during the warm summer periods from 1235 to 1305 and 1365 to 1407. In the 82 years between 1408 and 1491, severe winters followed each other every seven years, and in the 383 years between 1512 and 1895 every five and a half years. Less extreme events were not particularly noted by contemporaries. In the 20th century, there were still six severe winters between 1929 and 1963, whereby those between 1940 and 1942 – analogous to 1512 to 1514 – immediately followed each other (Pfister and Wanner, 2021). In terms of coldest temperatures and the duration of snow cover, the winters of 1077 (Wozniak, 2020), 1364, and 1573 can be classified as the most extreme. If the cold sum estimation is based on the occurrence and duration of frozen lakes bordering the Alps, the winter of 1573 may be in first place, unless Lake Brienz in the Bernese Oberland froze in 1364, as reported by a non-contemporary source (Pfister and Wanner, 2021). In Paris, the coldest winter within the instrumental period since 1659 was in 1830 (Rousseau, 2015). In the 20th century, severe winters became rarer with the exception of the very cold years 1929, 1956, and 1963. One could argue that a high number of extreme winters mainly occurred with the onset of the last three GSMs (Fig. 5d) and several volcanic clusters after about 1425 AD (Fig. 5c), but this date also marked the beginning of the period with a mostly negative NAO state (Fig. 5e). It is conceivable that internal variability in the form of negative NAO patterns played a decisive role in the development of very cold winters (Wanner et al., 2001 and Figs. 3e and f).

Extremely cold and warm summers are characterised by a specific oenological pattern. US oenologist Gregory V. Jones and environmentalist Robert E. Davis demonstrated that a large amount of the annual variation in vine harvest dates, crop sizes and sugar content is controlled by a handful of large-scale weather situations. In general, vine quality and quantity are reduced by high frequencies of cyclonic weather with cold fronts which also delay crop maturity. Conversely, a high occurrence of stable and warm anticyclonic weather situations increases the harvest size, improves the quality, and promotes the harvest date (Jones and Davis, 2000). This pattern is particularly evident in extremely hot and dry summers (Index +3; red series of dots in Fig. 5b) and in extremely cold and often wet "Years without a Summer" (Index -3; blue series of dots in Fig. 5b).

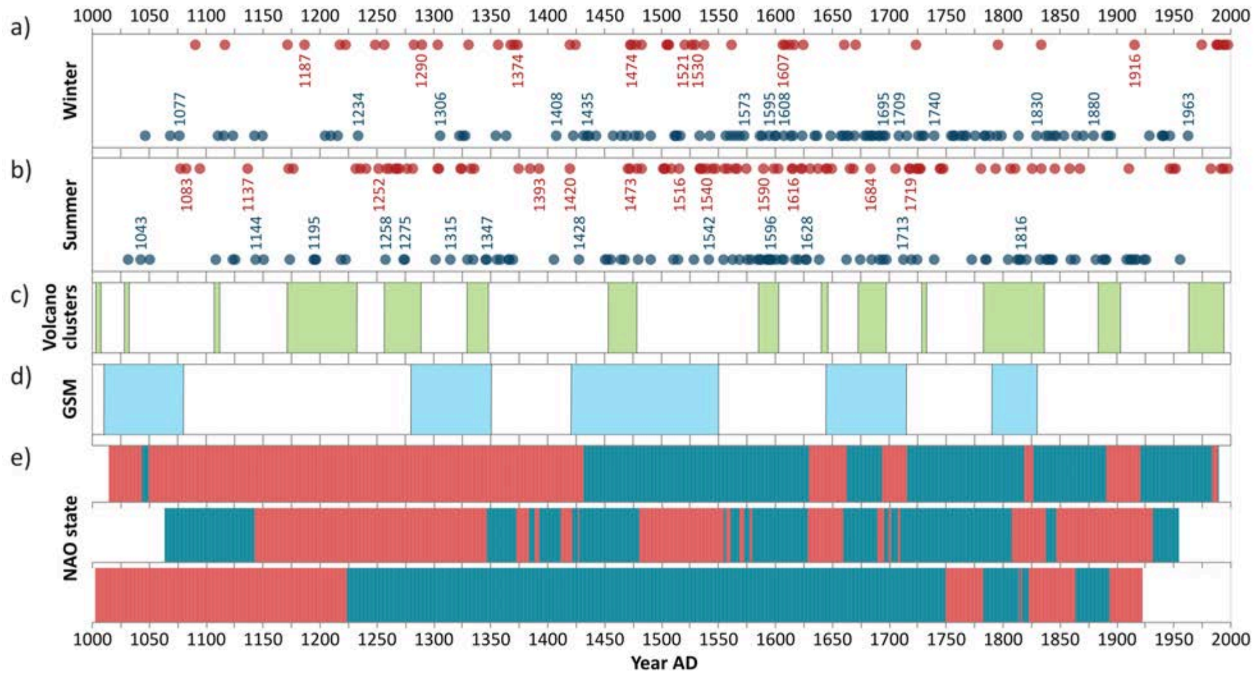

Figure 5. a) Extreme winters, indicated by Pfister Indices +3 (red) and -3 (blue). The most extreme events are marked with their corresponding year. b) Same, but for summer. c) Periods with clusters of volcanic eruptions (green; see Fig. 2a). d) Grand Solar Minima (blue; Oort, Wolf, Spörer, Maunder and Dalton Minimum). e) Three time series representing a positive (red) or negative (blue) NAO state (same curves as in Figure 2d).

Hot summers were quite frequent after 1225 AD. The longest and most torrid summers in the last 1000 years occurred in 1473 and 1540. Both were the culmination of a heat and drought period that lasted 14 months in 1473 and 11 months in 1540. In 1540 it affected an area from central Italy to the North Sea, from France to Poland (Pfister et al., 2018), and additionally included Ireland, Denmark, and southern Sweden in 1473 (Camenisch et al., 2020). While in the 19th century there were seven of these heatwaves, in the 20th century, before 1988, there were only five, and only the one in 1947 corresponds to the extremely hot summers in the Little Ice Age. This is confirmed by the homogeneous series of vintage data for Beaune, France, available from 1354 to 2018. The 33 extremely early harvests comprising the fifth percentile bracket of grape harvest days were unevenly distributed over time; 21 of them occurred between 1393 and 1719, while this is the case for just five years between 1720 and 2002 (Labbé et al., 2019). Interestingly, neither the volcanic and solar irradiance forcing nor the NAO state indicate a significant correlation with warm and dry summers.

Extremely wet and cold summers were relatively frequent in the 12th, 14th, 16th, 17th and 19th centuries, namely in the periods 1346–1370, 1576–1597, 1618–1639 and 1813–1864, which were accompanied by advances of the Alpine glaciers (Pfister and Wanner, 2021). Eight extremely cold summers were recorded in the 20th century, namely between 1912 and 1926, although none was as frosty as the "Years without a Summer" in the Little Ice Age. There is only a weak evidence that solar minima led to an increased frequency of cold summers (Fig. 3d), even though lower SSTs were probably registered (Gebbie and Huybers, 2019). In the case of the "Years without a Summer", massive volcanic eruptions are likely to have played a significant role (Fig. 3b). Typical examples following volcanic eruptions are 1258 (Samalas, Indonesia), 1596 (Nevado del Ruiz, Columbia?) and 1816 (Tambora, Indonesia). Brönnimann and Krämer (2016) use the Tambora outbreak of 1816 to document the totality of the dynamical processes that took place as well as the associated social effects.

5. Conclusions

Early studies of the LIA started in the Northern Hemisphere. This area is particularly sensitive to climate fluctuations due to the ice-albedo feedback and the coupled reaction of the Atlantic thermohaline circulation. Both the MCA (about 950-1250 AD) and LIA (about 1250-1860 AD) showed a high climate variability. On average the MCA was only a few tenths of a degree warmer than the LIA (Crowley and Lowery, 2000; Bradley et al., 2003; Mann et al., 2009). The transition between the two periods was complex and not continuous, and did not occur at the same time in different seasons and different regions. In general, the LIA was characterised by a high number of very cold winters, and the number of cold but also extremely warm summers was high. The latter was possibly induced by higher dryness and lower cloud cover(?).

The cooling of the LIA can be primarily attributed to increased volcanic activity and secondly to the reduced solar irradiance during several GSM. Both were coupled with dynamical processes in the higher atmosphere (reduced stratospheric ozone production, weakening of the polar vortex) and in the ocean (ice melt, weakening of the thermohaline circulation). The latter expressed itself in a tendency towards a negative NAO. It is possible that a slight cooling trend also occurred due to land use changes (loss of forest areas).

The beginning and end of the LIA are denoted very differently in the literature. Overall, the onset in the Southern Hemisphere is likely to have slowed down due to the inertia of the vast oceans. The end of the LIA began after the middle of the 19th century. Analyses and models show that, firstly, a warming occurred that was due to reduced volcanic activity and increased solar irradiance. In addition, the winter mass increase of the glaciers was reduced, and the concentration of greenhouse gases also increased slightly. The slow warming in the 20th century was mainly manifested in the decreased frequency and intensity of cold extreme events in summer and winter, while warm extremes remained rare until the transition to rapid warming after 1988.

The extreme events show at most a weak correlation with volcanic events and solar irradiance variability. Extremely cold winters are highly correlated with a negative NAO state, and cold-wet “Years without a Summer” were often the result of violent global volcanic eruptions.

Acknowledgements

We would like to expressly thank Tamara Bauman for producing the graphics. We thank Miryam Bar-Matthews, Ulf Büntgen and an anonymous reviewer for their very valuable comments.

Annex

Definition of periods with large volcanic eruptions (Fig. 2a) and Grand Solar Minima (Fig. 2b)

The volcanic periods in Figure 2 a were determined based on the data of Sigl et al. (2015). All years or short periods of a few years with a negative radiative forcing of less than -1 W/m2 were taken into account. If the eruptions were less than 25 years apart, they were combined into one group. This resulted in the following volcanic periods (years AD) for Figure 2 a: 1003 / 1028-1029 / 1108-1110 / 1171

- 1232 / 1257-1288 / 1329-1347 / 1453-1478 / 1585-1602 / 1641-1643 / 1673-1697 / 1729-1730 / 1783-1836 / 1883-1903 / 1963-1993.

The periods of the Grand Solar Minima (Fig. 2 b) are defined slightly differently by different authors (Steinhilber et al., 2009; Wu et al., 2018). We have chosen the following time periods, which are presented in this form in textbooks and on official websites (years AD): Oort 1010-1080, Wolf 1280-1350, Spörer 1420-1550, Maunder 1645-1715, Dalton 1790-1830.

Definition of the Pfister-Indices (Fig. 1b-e)

Ordinal-scale temperature indices are known to be a suitable approach to derive high resolution climate proxies from documentary data. Their evidence consists of narrative weather reports, documentary proxy data and early instrumental observations (Brönnimann et al. 2018). In the warm season this concerns phenological observations as well as data on the size and quality of grape harvests (Jones and Davies, 2000). In the cold season indices are mainly derived from observations of snow, ice cover and frost, as well as such about untimely spring vegetation. Until 1499 Pfister indices for very cold and very warm winters and summers (index -2, -3, +2 +3) are documented based on reliable compilations and calibrated documentary evidence. From 1500 to 1759 the indices were determined based on documentary-based estimates and subsequently from instrumental observations (Dobrovolný et al. (2010). The detailed proofs of the evidence underlaying Fig. 1 b-e can be downloaded from <DOI 10.7892/boris.148155> to which the following explanations refer. The seasonal Pfister indices for the whole period 1000 to 1999 are documented in Table 8 of this document.

For the period from 1000 to 1499 the indices -2, -3, +2 +3 for cold and warm seasons (without autumn) are proved from critical compilations and calibrated documentary evidence (Tables 1-5 of the document). The values for rather cold and rather warm as well as inconspicuous seasons (index -1, +1, 0) are proved in the chronological calibrations mentioned in Tables 2 and 3. For the period 1500 to 1759 the indices were derived from the seasonal temperature estimates and from the subsequent instrumental measurements (Dobrovolny et al., 2010) using the method of duodecile statistics (Table 6 and 7).

Indices +2, +3, -2 and -3 were assigned if the underlaying narrative weather reports and proxy data were meteorologically coherent. The validity of the approach can be illustrated using quasi analogues across the entire millennium, as it is shown below using examples for winter and summer taken from Pfister and Wanner (2021). Temperatures are related to deviations from the 1961-90 average. The following list presents examples:

Winter 1150, Index -3: Snow cover for 3 to 4 months in France and up to 6 months in Saxony. Frozen rivers (e. g. the Rhine) supported heavy cargoes. Many fruit trees and grapevines perished.
Winter 1408, Index -3: Frost from late November to February. Thick ice on major rivers and Lakes Zürich and Constance. Many people froze to death. Estimated temperature deviation -5.0° C (±0.69° C).
Winter 1830, Index -3: Cold-wave from early December to late February. Most rivers and lakes ice covered. Measured temperature deviation - 6.6° C.
Winter 1172, Index +3: It rained frequently and it only froze a day or two. Spring vegetation appeared very early and birds were singing and nesting.
Winter 1607, Index +3: Winds mainly from southwest. Rare snowfalls. Meadows full of flowers. People wore summer clothing. Estimated temperature deviation +3.6 ° C (±0.69° C)
Winter 1834, Index +3: Prevailing southwesterly winds and anticyclonic weather conditions, blossoming of spring flowers in January. Measured temperature deviation +2.7° C.
Summer 1144, Index -3: Cool conditions and persistent rain with westerly winds. Grape harvest small and of poor quality.

Summer 1621, Index-3: Rainy and very cold with frequent snowfall in the Alps. Grape harvests were very late, small and sour. Estimated temperature deviation -2.6° C (±0.49° C).

Summer 1821, Index-3: North-westerly winds with cool and rainy weather. Grape harvests very late, small and sour. Measured temperature deviation -2.2° C.

Summer 1304, Index +3: After a torrid spring, summer almost without rain. Level of large rivers very low. Abundant grape harvests of premium quality. Hot autumn.

Summer 1536, Index +3: Heat and drought from May to November. Frequent forest fires. Grape harvest early, abundant and sweet. Estimated temperature deviation +2.8° C (±0.49° C).

Summer 1947, Index +3: Warm season **t**emperatures above the long term mean with precipitation deficits. Early and abundant grape harvest of excellent quality. Measured temperature deviation + 1.9° C

References

Aagard, K. and Carmack, E.C., 1989. The role of sea ice and other fresh water in the arctic circulation. J. Geophys. Res. 94, 14485-14498.

Alonso-Garcia, M., Kleiven, H., McManus, J.F., Moffa-Sanchez, P., Broecker, W.S and Flower, B.B., 2017. Freshening of the Labrador Sea as a trigger for Little Ice Age development. Clim. Past 13, 317-331.

Anet, J.G., Rozanov, E.V., Muthers, S., Peter, T., Brönnimann, S., Arfeuille, F., Beer, J., Shapiro, A.I., Raible, C.C., Steinhilber, F. and Schmutz, W.K., 2013. Impact of a potential 21st century "grand solar minimum" on surface temperatures and stratospheric ozone. Geophys. Res. Lett. 40, 4420-4425.

Baker, A., Hellstrom J.C., Kelly B.F.J., Mariethoz, G. and Trouet, V., 2015. A composite annual-resolution stalagmite record of North Atlantic climate over the last three millennia. Sci. Rep. 5, 10307.

Bradley, R.S. and Jones, P.D., 1992. When was the "Little Ice Age"? In: Mikami, T. (ed.): Proceedings of the International Symposium on Little Ice Age Climate. Dept. of Geography, Tokyo Metropolitan University, Tokyo, 1-4 https://www.jstage.jst.go.jp.

Bradley, R.S., Hughes, M.K. and Diaz, H.F., 2003. Climate in Medieval Time. Science 302, 404-405.

Bradley R.S., Wanner, H. and, Diaz H.F., 2016. The medieval quiet period. Holocene 26(6), 990-993.

Braumann, S.M., Schafer, J.M., Neuhuber, S.M., Lüthgens, C., Hidy, A.J. and Fiebig, M., 2021. Early Holocene cold snaps and their expression in the moraine record of the eastern European Alps. Clim. Past 17, 2451-2479.

Brönnimann, S., Xoplaki, E., Casty, C., Pauling, A. and Luterbacher, J., 2007. ENSO influence on Europe during the last centuries. Clim. Dynam. 28(2), 181-197.

Brönnimann, S., Pfister, S., and White, S., 2018. Archives of Nature and Archives of Societies. In: White, S., Pfister, C. and Mauelshagen, F. (eds.). The Palgrave Handbook of Climate History, Palgrave Macmillan, London, 309-320.

Brönnimann, S., Franke, J., Nussbaumer, S.U., Zumbühl, H.J., Steiner, D., Trachsel, M., Hegerl, G.C., Schurer, A., Worni, M., Malik, A., Flückiger, J. and Raible, C.C., 2019. Last phase of the Little Ice Age forced by volcanic eruptions. Nat. Geosci. 12, 650-656.

Büntgen, U. and Hellmann, L., 2010. The Little Ice Age in scientific perspective: cold spells and caveats. J. Interdiscipl. Hist. 44(3), 353-368.

Büntgen, U., Myglan, V.S., Ljungqvist, F.C., McCormick, M., Di Cosmo, N., Sigl, M., Jungclaus, J., Wagner, S., Krusic, P.J., Esper, J., Kaplan, J.O., de Vaan, M.A.C., Luterbacher, J., Wacker, L., Tegel, W. and Kirdyanov, A.V., 2016. Cooling and societal change during the Late Antique Little Ice Age from 536 to around 660 AD. Nat. Geosci. 9(3), 1-7.

Camenisch, C., Brázdil, R., Kiss, A., Pfister, C., Wetter, O., Rohr, C., Contino, A. and Retsö, D., 2020. Extreme heat and drought in 1473 and their impacts in Europe in the context of the early 1470s. Reg. Environ. Change 20(1), doi:10.1007/s10113-020-01601-0.

Chen, J., Wan, G., Zhang, D.D., Chen, Z., Xu, J., Xiao, T. and Huang, R., 2005. The “Little Ice Age” recorded by sediment chemistry in Lake Erhai, southwest China. Holocene 15(6), 925-931.

Cook, E.R., Kushnir, Y., Smerdon, J.E., Williams, A.P., Anchukaitis, K.J. and Wahl, E.R., 2019. A Euro-Mediterranean tree-ring reconstruction of the winter NAO index since 910 C.E. Clim. Dynam. 53, 1567-1580.

Copard, K., Colin, C., Henderson, G.M., Scholten, J., Douville, E., Sicre, M.-A. and Frank, N., 2012. Late Holocene intermediate water variability in the northeastern Atlantic as recorded by deep-sea corals. Earth Planet. Sc. Lett. 313-314, 34-44.

Crowley, T J. and Lowery, T.S., 2000. How warm was the Medieval Warm Period? Ambio 29(1), 51-54.

Denton, G.H. and Karlén, W., 1973. Holocene climatic variations – their pattern and possible cause. Quaternary Res. 3, 155-205.

Deser, C., Phillips, A., Bourdette, V. and Teng, H., 2010. Uncertainty in climate change projections: the role of internal variability. Clim. Dynam. 38, 527-546.

Diaz, H.F., Trigo, R., Hughes, M.K., Mann, M.E., Xoplaki, E. and Barriopedro, D., 2011. Spatial and temporal characteristics of climate in Medieval times revisited. B. Am. Meteorol. Soc., Nov. 2011, 1487-1500.

Dickson, R.R., Meincke, J., Malmberg, S.A. and Lee, A.J., 1988. The Great Salinity Anomaly in the northern North Atlantic 1968-1982. Prog. Oceanogr. 20, 103-151.

Dobrovolný, P., Moberg A., Brázdil R., Pfister, C., Glaser, R., Wilson, R., van Engelen, A., Limanówka, D., Kiss, A., Halíčková, M., Macková, J., Riemann, D., Luterbacher, J. and Böhm, R., 2010. Monthly, seasonal and annual temperature reconstructions for Central Europe derived from documentary evidence and instrumental records since AD 1500. Climatic Change 101(1), 69-107.

Esper, J., Cook, E. R. and Schweingruber, F. H., 2002. Low-frequency signals in long tree-ring chronologies for reconstructing past temperature variability. Science 295, 2250-3.

Faust, J.C., Fabian, K., Milzer, G., Giraudeau, J. and Knies, J., 2016. Norwegian fjord sediments reveal NAO related winter temperature and precipitation changes of the past 2800 years. Earth. Planet. Sci. Lett. 435, 84-93.

Gebbie, G. and Huybers, P., 2019. The Little Ice Age and 2oth-century deep Pacific cooling. Science 363(6422), 70-74.

Grove, J. M., 1988. Little Ice Ages. Ancient and Modern. 2 Vols. Methuen, London, 718 S.

Helama S., Jones P.D. and Briffa K.R., 2017. Dark Ages Cold Period: A literature review and directions for future research. Holocene 27(10), 1600-1606.

Hernández, A., Sánchez-López, G., Pla-Rabes, S., Comas-Bru, L., Parnell, A., Cahill, N., Geyer, A., Trigo, R.M. and Giralt, S., 2020. A 2,000-year Bayesian NAO reconstruction from the Iberian Peninsula. Sci. Rep. 10:14961.

Holzhauser, H., Magny, M. and Zumbühl, H.J., 2005. Glacier and lake-level variations in west-central Europe over the last 3500 years. Holocene 15(6), 789-801.

Holzhauser, H., 2010. Zur Geschichte des Gornergletschers. Ein Puzzle aus historischen Dokumenten und fossilen Hölzern aus dem Gletschervorfeld. Geographisches Institut der Universität Bern, Bern, 253pp.

Ilyashuk, E.A., Heiri, O., Ilyshuk, B.P., Koinig, K.A. and Psenner, R., 2019. The Little Ice Age signature in a 700-year high-resolution chironomid record of summer temperatures in the Central Eastern Alps. Clim. Dynam. 52, 6953-6967.

Ineson, S., Maycock, A.C., Gray, L.J., Scaife, A.A., Dunstone, N.J., Harder, J.W., Knight, J.R., Lockwood, M., Manners, J.C., and Wood, R.A., 2015. Regional climate impacts of a possible future grand solar minimum. Nat. Commun. 6, no. 7535.

IPCC: Climate Change 2013, 2013.The Physical Science Basis. Contribution of Working Group I to the Fifth Assessment Report of the Intergovernmental Panel on Climate Change [Stocker T.F., Qin D., Plattner G.-K. et al. (eds.)]. Cambridge University Press, Cambridge, 1535 pp.

Jones, G.V. and Davis, R.E., 2000. Using a synoptic climatological approach to understand climate-viticulture relationships. Int. J. Climatol. 20(88), 813-837.

Jones, P.D. and Mann, M.E., 2004. Climate over past millennia. Rev. Geophys. 42, RG202.

Jones, P.D., Harpham, C. and Vinther, B.M., 2014. Winter-responding proxy temperature reconstructions and the North Atlantic Oscillation. J. Geophys. Res. Atmos. 119, 6497-6505.

Jouvet, G. and Huss, M., 2019. Future retreat of Great Aletsch Glacier. J. Glaciol. 65, 869-872.

Kaufman, D., McKay, N., Routson, C., Erb, M., Dätwyler, C., Sommer, P.S., Heiri, O. and Davis, B., 2020. Holocene global mean surface temperature, a multi-method reconstruction approach. Scientific Data 7, 201.

Labbé, T., Pfister, C., Brönnimann, S., Rousseau, D., Franke, J. and Bois, B., 2019. The longest homogeneous series of grape harvest dates, Beaune 1354-2018, and its significance for the understanding of past and present climate. Clim. Past 15, 1-17.

Lamb, H.H., 1965. The early medieval warm epoch and its sequel. Palaeogeogr. Palaeoecl. 1, 13-37.

Lamb, H.H., 1977. Climate: present, past and future, volume 2: Climatic history and the future. Methuen, London and New York, 855 pp.

Landsberg, H., 1985. Historical weather data and early meteorological observations. In: Hecht, A.D. (ed.): Paleoclimate Analysis and Modelling. John Wiley, New York, 27-70.

Lehner, F., Raible C.C. and Stocker, T.F., 2012. Testing the robustness of a precipitation proxy-based North Atlantic Oscillation reconstructions. Quaternary Sci. Rev. 45, 85-94.

Le Roy Ladurie, E., 1971. Histoire et Climat. Annales: Économies, Sociétés, Civilisations 14, no. 1, 3-34.

Le Roy Ladurie, E., 2012. Préface. In: Mer de glace, art et science. Editions Escope, Chamonix, 192pp.

Liu, Z., Zhu J., Rosenthal Y., Zhang, X., Otto-Bliesner, B.L., Timmermann, A., Smith, R.S., Lohmann, G., Zheng, W. and Oliver, E.T., 2014. The Holocene temperature conundrum. P. Natl. Acad. Sci. USA 111, E3501-E3505.

Lorenz, J., Jung-Hyun, K., Rimbu, N., Schneider, R. and Lohmann, G., 2006. Orbitally driven insolation forcing on Holocene climate trends: Evidence from alkenone data and climate modeling. Paleoceanography 21, PA1002.

Luterbacher, J., Koenig, S.J., Franke J. et al., 2010. Circulation dynamics and its influence on European and Mediterranean January–April climate over the past half millennium: Results and insights from instrumental data, documentary evidence and coupled climate models. Climatic Change 101,201–234.

Luterbacher J., Werner J.P., Smerdon J.E. et al., 2016. European summer temperatures since Roman times. Environ. Res. Lett. 11(2), doi: 10.1088/1748-9326/11/2/024001.

Ljungqvist F. C., 2010. A new reconstruction of temperature variability in the extra-tropical Northern Hemisphere during the last two millennia. Geogr. Ann. A. 92(3), 339-351.

Mangini, A., Spötl, C. and Verdes, P.F., 2005. Reconstruction of temperature in the Central Alps during the past 2000 yr from a $\delta^{18}O$ stalagmite record. Earth Planet. Sc. Lett. 235(3), 741-751.

Mann, M.E., Zhang, Z., Rutherford, S., Bradley, R.S., Hughes, M.K., Shindell, D., Ammann, C.M., Faluvegi, G. and Ni, F., 2009. Global signatures and dynamical origins of the Little Ice Age and Medieval Climate Anomaly. Science 326(5957), 1256-1260.

Marcott, S.A., Shakun, J.D., Clark, P.U. and Mix, A.C., 2013. A reconstruction of regional and global temperature for the past 11,300 years. Science 339 (6124), 1198–1201.

Martin-Puertas, C., Matthes, K., Brauer, A., Muscheler, R., Hansen, F., Christof, P., Aldahan, A., Possnert, G. and van Geel, B., 2012. Regional atmospheric circulation shifts induced by a grand solar minimum, Nat. Geosci. 5(6), 397-401.

Matthews J.A. and Briffa, K.R., 2005. The “Little Ice Age”: Re-evaluation of an evolving concept. Geogr. Ann. A. 87, 17-36.

Maycock, A.C., Ineson, S., Gray, L.J., Scaife, A.A.,Anstey, A.,Lockwood, M.,Butchart, N., Hardiman, S.C., Mitchell, D.M. and Osprey, S.M., 2015. Possible impacts of a future grand solar minimum on climate: Stratospheric and global circulation changes. J. Geophys. Res. Atmos. 120, 9043-9058.

Mayr, F., 1964. Untersuchungen über Ausmass und Folgen der Klima- und Gletscherschwankungen seit dem Beginn der postglazialen Wärmezeit. Z. Geomorphol., N.F. 8(3), 257-285.

Meehl, G.A., Arblaster, J.M. and Marsh, D.R., 2013. Could a future “grand solar minimum” like the Maunder Minimum stop global warming. Science 307, 1769-1772.

Miller G. H., Geirsdóttir Á., Yafang, Z., Larsen, D.J., Otto-Bliesner, B.L., Holland, M.M., Bailey, D.A., Refsnider, K.A., Lehman, S.J., Southon, J.R., Anderson, C., Björnsso, H. and Thordarson, T., 2012. Abrupt onset of the Little Ice Age triggered by volcanism and sustained by sea-ice/ocean feedbacks. Geophys. Res. Lett. 39, L02708.

Moffa-Sánchez, P., Hall, I. R., Barker, S., Thornalley, D.J.R. and Vashayaev, I., 2014. Surface changes in the eastern Labrador Sea around the onset of the Little Ice Age. Paleoceanography 29, 160-175.

Moore, J.J., Hughen, K.A., Miller, G.H. and Overpeck, J.T., 2001. Little Ice Age recorded in summer temperature reconstruction from varved sediments of Donald Lake, Baffin Island, Canada. J. Paleolimnol. 25, 503-517.

Moreno-Chamarro, E., Zanchettin, D., Lohmann, K., Luterbacher, J. and Jungclaus, J.H., 2017.Winter amplification of the European Little Ice Age cooling by the subpolar gyre. Nature Sci. Rep. 7, 9981.

Muscheler, R., Joos, F., Beer, J. et al., 2007. Solar activity during the last 1000 yr inferred from radionuclide records. Quat. Sci. Rev. 26(1-2), 82-97.

Mysak, L.A., Manak, D.K. and Marsden, R,F., 1990. Sea-ice anomalies observed in the Greenland and Labrador Seas during 1901-1984 and their relation to an interdecadal Arctic climate cycle. Clim. Dynam. 5, 111-133.

Nash, D.J., Adamson, C.D., Ashcroft, L., Bauch, M., Camenisch, C., Degroot, D., Gergis, J., Jusopovi, A., Labbé, T., Kuan-Hui, E.L., Nicholson, S.D., Qing, P., Rosario Prieto,M., Rack, U., Facundo, R. and White, S., 2021). Climate indices in historical climate reconstructions: a global state of the art. Clim. Past 17, 1273–1314.

Naveau, P., Nogaj, M., Ammann, C., Yiou, P., Cooley, D., and Jomelli, V., 2005. Statistical methods for the analysis of climate extremes. C. R. Geosciences 337, 1013-1022.

Neukom, R., Gergis, J., Karoly, D J. et al., 2014. Inter-hemispheric temperature variability over the past millennium. Nat. Clim. Change 4, 362-367.

Nieto-Moreno, V., Martinez-Ruiz, F. and Giralt, S., 2013. Climate imprints during the 'Medieval Climate Anomaly' and the 'Little Ice Age' in marine records from the Alboran Sea basin. Holocene 23(9), 1227-1237.

Nussbaumer, S. U., Huss, M., Machguth, H. and Steiner, D., 2016. Gletscherentwicklung und Klimawandel. Von der Vergangenheit in die Zukunft. In: Zumbühl, H. J., Nussbaumer, S. U., Holzhauser, H. and Wolf, R. (eds.). Die Grindelwaldgletscher. Kunst und Wissenschaft, Haupt, Bern, 215-234.

Oerlemans J., 2005. Extracting a climate signal from 169 glacier records. Science 308, 675-677.

Ogilvie, A. E. J. and Jónsson, T., 2001. "Little Ice Age" research: a perspective from Iceland. Climatic Change 48, 9-52.

Oliva, M., Ruiz-Fernández, J., Barriendos, M. et al., 2018. The Little Ice Age in Iberian mountains. Earth-Sci. Rev. 177, 175-208.

Olsen, J., Andersen, N.J. and Knudsen, M.F., 2012. Variability of the North Atlantic Oscillation over the past 5,200 years. Nat. Geosci. 5, 808-812.

Ortega, P., Lehner, F., Swingedouw, D., Masson-Delmotte, V., Raible, C.C., Casado, M. and Yiou, P., 2015. A model-tested North Atlantic Oscillation reconstruction for the past millennium. Nature 523, 71-74.

Osman, M. B., Tierney, J. E., Zhu, J., Tardif, R., Hakim, G. J., King, J. and Poulsen, C. J., 2021. Globally resolved surface temperatures since the Last Glacial Maximum. Nature 599, 239-244.

Otto-Bliesner, B.L., Brady, E.C., Fasullo, J., Jahn, A., Landrum, L., Stevenson, S., Rosenbloom, N., Mai, A. and Strand, G., 2016. Climate variability and change since 850 CE: an ensemble approach with the community earth system mode. Bull. Am. Meteorol. Soc. 97, 735-754.

Owens, M.J., Lockwood, M., Hawkins, E., Uusoskin, I., Jones, G.S., Barnard, L., Schurer, A and Fasullo, J., 2017. The Maunder minimum and the Little Ice Age; an update from recent reconstructions and climate simulations. J. Space Weather Space Clim. 7, A33, https://doi.org/10.1051/swsc/2017034.

Pfister, C., 2007. Little Ice Age-Type Impacts and the Mitigation of Social Vulnerability to Climate in the Swiss Canton of Bern Prior to 1800. In: Costanza Robert, Graumlich Lisa, Steffen Will (eds.). Sustainability of Collapse? An Integrated History and Future of People on Earth, MIT Press, Cambridge (MA), 197-212.

Pfister, C., Camenisch, C., and Dobrovolný, P., 2018. Analysis and Interpretation: Temperature and Precipitation Indices. In: The 1500 Palgrave Handbook of Climate History, White, S., Pfister, C., and Mauelshagen, F. (Eds.), Palgrave-Macmillan, London, 115-129.

Pfister, C. and Wanner, H., 2021. Climate and Society in Europe. The Last Thousand Years. Haupt, Bern, 397 pp.

Pinto, J.G. and Raible, C. C., 2012. Past and recent changes in the North Atlantic oscillation. Wiley Interdisciplinary Reviews: Climate Change 3 (1), 79-90.

Porter, S.C., and Denton, G.H., 1967. Chronology of neoglaciation in the North American Cordillera. Am. J. Sci. 265, 177-210.

Reichert, B. K., Bengtsson, L. and Oerlemans, J., 2001. Midlatitude forcing mechanisms for glacier mass balance investigated using general circulation models. J. Climate 14(17), 3767-3784.

Robock, A., 2000. Volcanic eruptions and climate. Rev. Geophys. 38(2), 191-219.

Rousseau, D., 2015. Fluctuations des dates de vendages Bourgignonnes et fluftuations des températures d'Avril à Septembre de 1378 à 2010. XXVIIe Colloque de l'Association Internationale de Climatologie, 2-5 Juillet 2014 – Dijon (France), 757-763.

Scaife, A.A., Knight, J.R., Vallis G.K. and Folland, C.K., 2005. A stratospheric influence on the winter NAO and North Atlantic surface climate. Geophys. Res. Lett. 32, L18715.

Sigl, M., Winstrup, M., McConnell, J. R. et al., 2015. Timing and climate forcing of volcanic eruptions for the past 2,500 years. Nature 523, 543-549.

Sigl, M., Abram, N.J., Gabrieli, J., Jenk, T.M., Osmont, D. and Schwikowski, M., 2018. 19th century glacier retreat in the Alps preceded the emergence of industrial black carbon deposition on high-alpine glaciers. Cryosphere 12, 3311-3331.

Solomina, O.N., Bradley, R.S., Hodgson, D.A., Ivy-Ochs, S., Jomelli, V. et al., 2015. Holocene glacier fluctuations. Quat. Sci. Rev. 111, 9-34.

Steiner, D., Pauling, A., Nussbaumer, S. U. et. al., 2008. Sensitivity of European glaciers to precipitation and temperature - two case studies. Climatic Change 90(4), 413-441.

Steinhilber, F., Beer, J. and Fröhlich C., 2009. Total solar irradiance during the Holocene. Geophys. Res. Lett. 36 (19).

Sutton, R.T., McCarthy, G.D., Robson, J., Sinha, B., Archibald, A.T. and Gray, L., 2018. Atlantic multidecadal variability and the U.K. ACSIS program. B. Am. Meteorol. Soc. 99, 415-425.

Toohey, M. and Sigl, M., 2017. Volcanic stratospheric sulfur injections and aerosol optical depth from 500 BCE to 1900 CE. Earth Syst. Sci. Data 9, 809-831.

Trouet, V., Esper, J., Graham, N. E., Baker, A., Scourse, J. D., and Frank, D., 2009. Persistent positive North Atlantic oscillation mode dominated the Medieval Climate Anomaly. Science 324(5923), 78-80.

Trouet, V., Scourse, J. D. and Raible, C., 2012. North Atlantic storminess and Atlantic Meridional Overturning Circulation during the last Millennium: Reconciling contradictory proxy records of NAO variability. Global Planet. Change 84-85, 48-55.

Usoskin, I. G., Gauthier, H., Gallet Y. et al., 2014. Evidence for distinct modes of solar activity. Astron. Astrophys. L10, doi:10.1051/ooo4-6361/201423391.

Walsh, J.E. and Chapman, W.L., 1990. Arctic contribution to upper-ocean variability in the North Atlantic. J. Climate 3, 1467-1473.

Wanner, H., 2021. Late Holocene: Cooler or warmer. Holocene 31(9).

Wanner, H., Holzhauser, H., Pfister, C., und Zumbühl H. J., 2000. Interannual to century scale climate variability in the European Alps. Erdkunde 54, 62-69.

Wanner, H., Brönnimann, S., Casty, C., Gyalistras, D., Luterbacher, J., Schmutz, C., Stephenson, D. B. and Xoplaki, E., 2001. North Atlantic Oscillation – concepts and studies. Surv. Geophys. 22, 321-382.

Wanner H., Beer J., Bütikofer J. et al., 2008. Mid- to Late Holocene climate change: An overview. Quaternary Sci. Rev. 27(19-20), 1791-1828.

Wanner, H. and Grosjean, M., 2014. Globale Temperaturvariabilität der letzten 2000 Jahre. Physik in unserer Zeit 4/2014, 176-180.

Wanner, H., 2021. Late Holocene: Cooler or warmer? Holocene 31(9), 1501-1506

Wassenburg, J.A., Immenhauser, A., Richter, D.K., Noedermayr, A., Riechelmann, S., Fietzke, J. Scholz, D., Jochum,K.P., Fohlmeuster, J., Schröder-Ritzrau, A., Sabaoui, A., Riechelmann, D.F.C., Schneider, L. and Esper, J., 2013. Moroccan speleothem and tree ring record suggest a variable positive state of the North Atlantic Oscillation during the Medieval Warm Period. Earth Planet. Sc. Lett. 375, 291-302.

White, W. B., Lean, J., Cayan, D. R. and Dettinger, M. D., 1997. Response of a global upper ocean temperature to changing solar irradiance. J. Geophys. Res. Atmos. 102 (C2), 3255-3266.

Wozniak, T., 2020. Naturereignisse im frühen Mittelalter. Das Zeugnis der Geschichtsschreibung vom 6. Bis 11. Jahrhundert. De Gruyter, Berlin, 970pp.

Wu, C.J., Usoskin, I.G., Krivova, N., Kovaltsov, G.A., Baroni, M., Bard, E. and Solanki, S.K., 2018. Solar activity over nine millennia: A consistent multi-proxy reconstruction. Astron. Astrophys. 615, A93, 1-13.

Zumbühl, H. J., Steiner, D. and Nussbaumer, S. U., 2008: 19th century glacier representation and fluctuations in the central and western European Alps: an interdisciplinary approach. Global Planet. Change 60(1-2), 42-57.

Zumbühl, H. J., 2016. Die eÿss schropfen so wachsen und schwynen. Die Geschichte des Unteren Grindelwaldgletschers seit dem 12. Jahrhundert. In: Zumbühl, H. J., Nussbaumer, S., Holzhauser, H. and Wolf, R. (eds.). Die Grindelwaldgletscher. Kunst und Wissenschaft. Haupt, Bern, 45-114.